THE GEOLOGICAL SOCIETY
OF AMERICA®

Coupled oceanic oxygenation and metazoan diversification during the early–middle Cambrian?

Chao Li[1]*, Chengsheng Jin[1], Noah J. Planavsky[2], Thomas J. Algeo[1,3,4], Meng Cheng[1], Xinglian Yang[5], Yuanlong Zhao[5], and Shucheng Xie[1]

[1]State Key Laboratory of Biogeology and Environmental Geology, China University of Geosciences, Wuhan 430074, China
[2]Department of Geology and Geophysics, Yale University, New Haven, Connecticut 06520, USA
[3]State Key Laboratory of Geological Processes and Mineral Resources, China University of Geosciences, Wuhan 430074, China
[4]Department of Geology, University of Cincinnati, Cincinnati, Ohio 45221-0013, USA
[5]College of Resource and Environment, Guizhou University, Guiyang 550003, China

ABSTRACT

The early–middle Cambrian (Fortunian to Age 4) is characterized by a significant increase in metazoan diversification. Furthermore, this interval is marked by a prominent environmental and ecological expansion of arthropod- and echinoderm-rich biotas. Recent redox work has suggested that this shift occurred during stable or decreasing marine oxygen levels, suggesting that these paleobiological and paleoecological transformations were decoupled from a redox control. We tested this idea by conducting new paleoredox analyses on Age 2–Age 4 Cambrian outer shelf (Jiuqunao-Wangjiaping), slope (Wuhe-Geyi), and basinal (Zhalagou) sections of the South China Craton. Multiple sections indicate that mid-depth waters transitioned from anoxic conditions during Cambrian Age 2 to stable oxic conditions during Cambrian Age 4. These findings suggest a stepwise expansion of oxic waters from shallow to deep settings during the early–middle Cambrian, consistent with a redox control of metazoan diversification and ecological expansion. More broadly, despite the surge in redox work over the past decade, this study highlights the need for continued coupled redox and paleontological studies to directly test models about the links between the evolution of animals, ecosystems, and marine redox conditions.

INTRODUCTION

During the early–middle Cambrian Period (Fortunian to Age 4) there was an explosion of metazoan diversity, including the appearance of small shelly faunas and more complex biotas dominated by arthropods and echinoderms (e.g., the Chengjiang Biota; Zhu et al., 2006). Although the record of early metazoan evolution is increasingly well understood, the underlying cause of these biotic events continues to be debated. Global redox changes (i.e., rapid rise or fall in atmospheric and oceanic oxygen levels) have been widely proposed; for example, the rapid rise of metazoan morphologic and taxonomic diversity during the early–middle Cambrian has been attributed to increasing atmospheric and oceanic oxygen levels (Knoll and Carroll, 1999; Chen et al., 2015b; Jin et al., 2016). However, the links between metazoan evolution and environmental oxygenation may have been complex or weak. A recent study suggested a decline in atmospheric and oceanic oxygen levels during Cambrian Age 3–Age 4 linked to rising bioturbation intensity beginning in Cambrian Age 2 (Boyle et al., 2014). Another study suggested static marine oxygen levels and dominantly anoxic conditions in all Cambrian based on statistical analysis of global iron speciation data (Sperling et al., 2015). Given this debate, new studies of early–middle Cambrian shallow to deep ocean systems are needed to evaluate the relationships among metazoan evolution, ecosystem structure, and ocean oxygenation.

We conducted a high-resolution Fe-trace element geochemical study of lower-middle Cambrian (Fortunian to Age 4) sections of the South China Craton representing intermediate- to deep-marine settings, including outer shelf (Jiuqunao-Wangjiaping, JW; note: Jiuqunao data were compiled from Och et al. [2016]), slope (Wuhe-Geyi, WG), and basinal (Zhalagou, ZLG) sections of the Yangtze Block (Fig. DR1 in the GSA Data Repository[1]). Linking our redox proxy analysis with detailed paleontological data from the lower-middle Cambrian of South China affords the unique opportunity to investigate the association, if any, between ocean-redox evolution and metazoan diversification during the early to middle Cambrian in South China and possibly elsewhere.

LITHOSTRATIGRAPHY AND STRATIGRAPHIC CORRELATION

The lower-middle Cambrian succession at JW (30°53′0.93″N, 110°52′47.25″E for Jiuqunao, 30°48′41″N, 111°11′12″E for Wangjiaping) comprises, moving upsection, the Yanjiahe, Shuijingtuo, Shipai, and Tianheban Formations (Fig. 1A). The upper Yanjiahe, uppermost Shuijingtuo, and Tianheban Formations consist mainly of limestones, whereas the Shuijingtuo and Shipai Formations are mainly black shales, mudstones, and siltstones. The lower-middle Cambrian succession at WG (26°45′34″N, 108°24′33″E for Wuhe, 26°48′12″N, 108°14′10″E for Geyi) comprises the upper Liuchapo, Jiumenchong, Bianmachong, and Balang Formations (Fig. 1B). The section consists mainly of black shales, mudstones, and siltstones, although phosphatic chert is present in the upper Liuchapo Formation and muddy limestones are present in the upper Jiumenchong Formation. The lower-middle Cambrian succession at ZLG (25°59′6″N, 107°53′32″E) consists of the Laobao, Zhalagou, and Duliujiang Formations (Fig. 1C). The Zhalagou and Duliujiang Formations are black shales, and the upper Laobao Formation is phosphatic chert.

Correlations among the study sections are based on radiometric ages and extensive biostratigraphic work. The key tiepoints among sections are shown in Figure 1. The lowermost Cambrian black shale layer, which is a correlation marker across the Yangtze Platform, has been dated to early Cambrian Age 2 based on zircon U-Pb ages: 526.4 ± 5.4 Ma at Wuhe-Aijiahe, ~20 km from the JW section (Okada et al., 2014), and 522.3 ± 3.7 Ma at Bahuang, ~80 km from the WG section (Chen et al., 2015a). The upper Shuijingtuo Formation at JW and the upper Jiumenchong Formation at WG are dated to early Cambrian Age 3 based on the trilobite *Hupeidiscus orientalis* (Yang et al., 2016). The basal Shipai Formation at JW and uppermost Jiumenchong Formation at WG are constrained to

*E-mail: chaoli@cug.edu.cn

[1]GSA Data Repository item 2017245, detailed geological settings, analytical methods, and supplemental figures and data tables, is available online at http://www.geosociety.org/datarepository/2017/, or on request from editing@geosociety.org.

GEOLOGY Data Repository item 2017245 | doi:10.1130/G39208.1

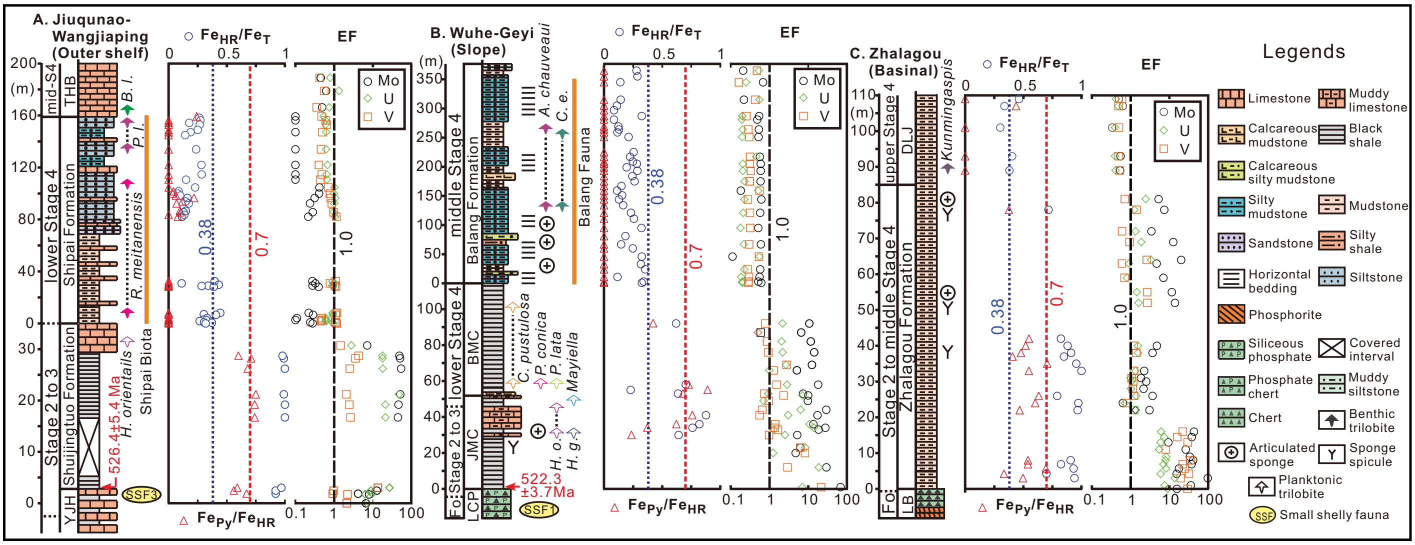

Figure 1. Lithostratigraphic columns, U-Pb ages, fossil records, and chemostratigraphy of the lower–middle Cambrian Jiuqunao-Wangjiaping, Wuhe-Geyi, and Zhalagou sections of the Yangtze Block (South China). Note that Jiuqunao-Wangjiaping and Wuhe-Geyi are composite sections, and that all chemostratigraphic data except for those at Jiuqunao (Och et al., 2016) are original to this study. Fo—Fortunian; mid-S4—middle Stage 4; EF—enrichment factor, Fe_{HR}/Fe_T (highly reactive iron/total iron) and Fe_{Py}/Fe_{HR} (pyrite iron/highly reactive iron). Formations: LCP—Liuchapo, JMC—Jiumenchong, BMC—Bianmachong, YJH—Yanjiahe, THB—Tianheban, LB—Laobao, DLJ—Duliujiang. Fossils: *H.—Hupeidiscus, R.—Redlichia, P. l.—Palaeolenus lantenosis, B.l.—Brevíredlichia liantuoensis, H. o.—H. orientails, H. g.—H. guizhougensis, C.—Chengkouia, P.—Protolenella, A.—Arthricocepalus, C. e.—Changaspis elongata*.

early Age 4 of the middle Cambrian (ca. 514–509 Ma) based on the trilobites *Redlichia meitanensis* and *Mayiella* (Yang et al., 2016). This age framework is confirmed by the trilobites *Breviredlichia liantuoensis* in the basal Tianheban Formation at JW and *Arthricocephalus chauveaui* in the middle Balang Formation at WG, which belong to the *Megapalaeolenus* Zone of middle Age 4 (Yuan and Zhao, 1999; Na and Kiessling, 2015). The trilobite *Kunmingaspis*, found in the basal Duliujing Formation at ZLG, belongs to the latest *Chittidilla plana–Paragraulos kunmingensis* trilobite Zone, demonstrating an age of late Age 4 for the lower part of that unit (Yuan and Zhao, 1999; Na and Kiessling, 2015).

GEOCHEMICAL PROXIES FOR MARINE REDOX CONDITIONS

Iron speciation is a widely used paleoredox proxy that, based on analysis of reactive iron phases in siliciclastic rocks, can track local water-column redox conditions (cf. Poulton and Canfield, 2011). Iron speciation is an empirically calibrated proxy, and therefore care must be taken when selecting samples. However, Fe speciation is one of the most extensively explored proxies and is robust when examined rocks are lithologically similar to those in the calibration studies. In modern and ancient oxic marine sediments the ratio of highly reactive iron (Fe_{HR}) to total Fe (Fe_T), i.e., Fe_{HR}/Fe_T, is commonly <0.38. In contrast, Fe_{HR}/Fe_T values exceeding this threshold are indicative of sediments deposited under anoxic conditions. When anoxia is indicated, the ratio between pyrite iron (Fe_{Py}) and Fe_{HR} provides evidence for ferruginous ($Fe_{Py}/Fe_{HR} < 0.7–0.8$) versus euxinic conditions ($Fe_{Py}/Fe_{HR} > 0.7–0.8$).

In order to validate paleoredox interpretations based on Fe speciation data, enrichments of redox-sensitive trace elements (RSTEs) (expressed as enrichment factors, or EFs) can be used as an independent proxy. RSTEs tend to be less soluble and more particle reactive under reducing conditions than under oxidizing conditions, leading to authigenic enrichments in anoxic facies (Algeo and Maynard, 2004). Mo is present in oxic water masses mainly as the conservative molybdate anion (MoO_4^{2-}), which is converted to particle-reactive thiomolybdates ($MoO_{4-x}S_x^{2-}$, x = 1–4) through reaction with H_2S under sulfidic conditions. U is present in seawater mainly as soluble U(VI) under oxic conditions, but is reduced to less soluble U(IV) under anoxic conditions. Transfer of seawater V to the sediment is associated with a two-step reduction process in which V(V) is converted to V(IV) under mildly reducing conditions and further to V(III) under euxinic conditions.

Detailed descriptions of the analytical methods for iron speciation, trace metals, other geochemical analyses, and statistical tests used in this study are provided in the Data Repository.

EARLY–MIDDLE CAMBRIAN MARINE REDOX CONDITIONS

In the outer shelf JW section (Fig. 1A), Age 2–Age 3 (uppermost Yanjiahe and Shuijingtuo Formations) samples are characterized by high Fe_{HR}/Fe_T (0.92–1.00) and moderate to high Fe_{Py}/Fe_{HR} (0.56–0.75), indicating ferruginous to euxinic conditions. Reducing conditions are supported by enrichments factors of 45 (7–52) for Mo and 18 (7–23) for U (note that reported values are the median and 16th–84th percentile range). V exhibits lower enrichment factors (2.3; 1.3–3.7) similar to that reported for ferruginous and euxinic units of Ediacaran age (e.g., Sperling et al., 2016). All Age 4 (Shipai and Tianheban Formations) samples are characterized by low Fe_{HR}/Fe_T (0.08–0.44) and low Fe_{Py}/Fe_{HR} (0–0.62), suggesting oxic depositional conditions. This inference is consistent with low Mo_{EF} (0.3 ± 0.2; mean ± SD), U_{EF} (0.8 ± 0.2), and V_{EF} (0.7 ± 0.3) in the Age 4 formations.

In the slope WG section (Fig. 1B), available Age 2 to early Age 4 (Jiumenchong and Bianmachong Formations) samples have variable Fe_{HR}/Fe_T (0.23–0.88) and variable Fe_{Py}/Fe_{HR} (0.24–0.89), indicating dominantly ferruginous conditions punctuated by episodic euxinia. In contrast, all older Age 4 (Balang Formation) samples show low Fe_{HR}/Fe_T (0.08–0.35) and low Fe_{Py}/Fe_{HR} (~0), suggesting oxic depositional conditions, consistent with low Mo_{EF} (0.5 ± 0.2), U_{EF} (0.3 ± 0.1), and V_{EF} (0.3 ± 0.1). This is also consistent with trace metal enrichment patterns: samples from the lower member (0–29 m) show greater enrichments [Mo_{EF} = 18 (5–50), U_{EF} = 8 (4–14), V_{EF} = 7 (4–15)] than samples from the upper member (29–92 m) [Mo_{EF} = 12 (7–18), U_{EF} = 2.3 (1.0–6.8), V_{EF} = 1.0 (0.7–1.6)]. These small enrichments are consistent with sulfide restricted to sediment pore waters (cf. Scott and Lyons, 2012).

In the basinal ZLG section (Fig. 1C), available Age 2 to middle Age 4 (Zhalagou Formation) samples have relatively high Fe_{HR}/Fe_T (0.70–1.00) and relatively low Fe_{Py}/Fe_{HR} (0.33–0.71), indicative of dominantly ferruginous conditions. This redox interpretation is in agreement with the moderate trace metal enrichments of the lower member (0–20 m) of the Zhalagou Formation [Mo_{EF} = 35 (16–42), U_{EF} = 7 (6–9), V_{EF} = 27 (19–54)], and with the reduced trace metal enrichments of the middle member (20–50 m; Mo_{EF} 2.7 ± 1.2, U_{EF} 1.2 ± 0.3, V_{EF} 1.2 ± 0.2) and upper member (50–85 m; Mo_{EF} 9.6 ± 5.5, U_{EF} 1.7 ± 0.8, V_{EF} 1.4 ± 1.0). Given Mo concentrations as high as hundreds of parts per million in some Cambrian black shales of South China (Jin et al., 2016), the small Mo enrichments in the middle and upper members may have resulted from low H_2S concentrations (<10 µm) that limited the formation of thiomolybdates (e.g., Erickson and Helz, 2000). In contrast, all late Age 4 (Duliujiang Formation) samples have low Fe_{HR}/Fe_T (0.30–0.46) and low Fe_{Py}/Fe_{HR} (0–0.44), suggesting dominantly oxic conditions, consistent with extremely low Mo_{EF} (0.5 ± 0.1), U_{EF} (0.4 ± 0.0), and V_{EF} (0.5 ± 0.0).

In summary, our results suggest that the outer shelf to basinal facies of the Yangtze Block, which were initially anoxic, transitioned to more oxygenated conditions during Cambrian Age 3–Age 4 (Fig. 2C). During the first increase, at the end of Age 3 or the beginning of Age 4 (ca. 514 Ma), anoxia yielded to oxic conditions at the outer shelf JW section. During the second increase, in middle Age 4, persistently oxic conditions expanded from outer shelf to slope areas (e.g., WG), although basinal settings (e.g., ZLG) remained dominantly anoxic at that time. In late Age 4, oxic waters expanded from slope to basinal environments (e.g., ZLG). Our new results demonstrate that deeper waters on the Yangtze Block remained anoxic during Age 3, and that an additional stepwise rise of oxygen levels occurred from Age 3 to Age 4. There is no obvious sedimentological evidence to indicate that transitions were linked to changes in sedimentation rates or depositional facies that shut off a reactive iron or RSTE trap (e.g., the entire ZLG section is characterized by uniform mudstone deposition; Fig. 1C).

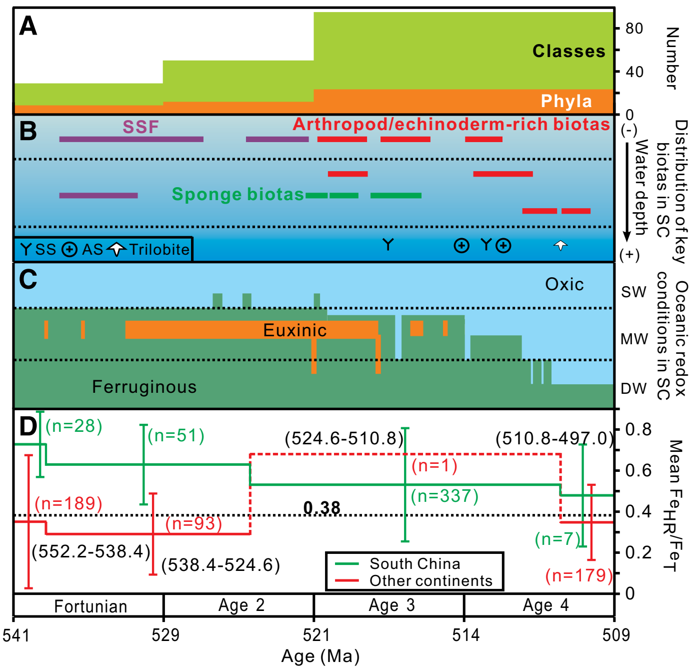

Figure 2. Marine redox and biodiversity patterns of the early–middle Cambrian. A: Number of phyla and classes globally (Erwin et al., 2011). B: Spatiotemporal distribution of key biotas in South China, including biotas dominated by small shelly faunas, sponges, and arthropods and echinoderms (Zhu, 2010). C: Spatiotemporal variation in ocean redox conditions in South China (this study; Jin et al., 2016, and references therein). D: Comparison of mean Fe_{HR}/Fe_T (highly reactive iron/total iron) ratios in four time bins between South China database and other continent databases. This statistical analysis includes only samples from outer shelf and basinal environments. The four time bins are divided by the major changing points of full Fe_{HR}/Fe_T data identified through a single-point detection test (see the Data Repository [see footnote 1]). The sample number and time range of each bin are shown in brackets. Each whisker represents the standard error. Abbreviations: SSF—small shelly fauna, SS—sponge spicule, AS—articulated sponge, SC—South China, SW—surface waters, MW—mid-depth waters, DW—deep waters.

With the addition of our new data, increasing oceanic oxygenation during Cambrian Age 2–Age 4 becomes statistically evident in the full South China deep-water Fe speciation database (Table DR4), as shown by a progressive decline of mean Fe_{HR}/Fe_T from 0.73 in the Fortunian to 0.43 in Age 4 [see Fig. 2D; $p < 0.05$ for ANOVA (analysis of variance) and Kruskal-Wallis tests; Table DR1]. This is in marked contrast to the mostly unchanged average redox conditions for the same interval (mean Fe_{HR}/Fe_T < 0.38 but $p > 0.05$; Table DR2) suggested by available Fe speciation data from other continents (Fig. 2D; Table DR4). In addition, we conducted a single-point detection test (using the R package Changepoint; https://cran.r-project.org/web/packages/changepoint/changepoint.pdf) with published global deep-water iron speciation data from 635 to 497 Ma (Table DR4), in which each iron speciation value was assigned an age based on available age constraints in order to create a time series. Using this approach, the most significant change in Fe_{HR}/Fe_T ratios occurred at 514 Ma (see Fig. DR3). Despite these statistical results, we stress that a dearth of early-middle Cambrian units in the database renders uncertain whether the pattern that we observe for South China, i.e., stepwise oceanic oxygenation during Cambrian Age 2–Age 4, represents a global phenomenon. Our results should provide motivation for additional redox studies of other early-middle Cambrian continental margins with paleodepth constraints.

Our findings allow for a reevaluation of some of the current controversies surrounding atmospheric and oceanic oxygen levels during the early–middle Cambrian.

(1) Sperling et al. (2015) found no evidence for discrete oxygenation events during the Ediacaran–Cambrian Periods based on a statistical analysis of global Fe speciation data. The conflict with our results may be related to the scale of investigation: our study makes use of considerably more Age 3–Age 4 Fe speciation data from deeper water settings, facilitating recognition of redox shifts during this interval.

(2) Boyle et al. (2014) proposed a decline in atmospheric and oceanic oxygen levels during Cambrian Age 3–Age 4 resulting from reduced organic burial related to intensified bioturbation beginning in Cambrian Age 2. Our results refute such a decline in oxygen levels, in agreement with recent work suggesting that bioturbation intensity did not rise significantly during the early Cambrian (Tarhan et al., 2015).

EARLY–MIDDLE CAMBRIAN OCEAN OXYGENATION AND METAZOAN EVOLUTION

Our finding of stepwise oceanic oxygenation in South China during Cambrian Age 2–Age 4 provides new insights into environmental controls on early metazoan evolution. For example, this stepwise oceanic oxygenation corresponds temporally to the regional replacement in South China of small shelly faunas and sponge-dominated communities (Fortunian and Age 2) by more complex arthropod- and echinoderm-rich biotas (Age 3 and Age 4) (Figs. 2B and 2C; Peng et al., 2005). Given the relatively high respiratory oxygen demands of echinoderms and mobile metazoans like arthropods, rising oceanic oxygen levels are likely to have facilitated the diversification of metazoans during Age 2–Age 3 (Sperling et al., 2013). Furthermore, a spatial expansion of marine invertebrates is recorded in South China during Cambrian Age 3–Age 4, as evidenced by (1) the stepwise expansion of complex arthropod-dominated biotas from shallow-shelf to deep-slope facies (Fig. 2B), and (2) the invasion of deep-water habitats by sponges, echinoderms, and trilobites (Fig. 2B; Peng et al., 2005; Smith et al., 2013). Collectively, these observations support a pronounced redox control on early metazoan ecology.

Rising oceanic oxygen levels in South China during Age 2 and early Age 3 also coincided with regional increases in the diversity of basic metazoan body plans (i.e., numbers of classes and phyla) (Fig. 2A), providing evidence for causal links between these factors, as hypothesized by Knoll and Carroll (1999). However, the lack of major body plan diversification (in South China and globally; Erwin et al., 2011) during Age 3–Age 4, which was the key interval of oxygenation in South China (>12 m.y.; Fig. 2A), casts doubt on the Knoll and Carroll (1999) model. Alternatively, the initial appearance of morphologically (and functionally) complex, metabolically demanding metazoan body plans may not have been immediately followed by a radiation of representative taxa; there was likely a slow transition between morphological innovation and ecologically meaningful implementation (e.g., Erwin et al., 2011). In this case, environmental factors such as oceanic redox state may have played an important role in the widespread implementation of ecological innovations.

CONCLUSIONS

Our Fe-trace element geochemical study of Cambrian Age 2–Age 4 strata in the outer shelf (Jiuqunao-Wangjiaping), slope (Wuhe-Geyi), and basinal (Zhalagou) sections of the Yangtze Block indicates a stepwise expansion of oxic waters from shallow- to deep-marine settings during the early–middle Cambrian. These findings differ from the results of earlier studies that inferred stable or decreasing oceanic oxygen levels at that time (Boyle et al., 2014; Sperling et al., 2015). Coupling our redox proxy work with detailed lower–middle Cambrian paleontological records from South China suggests that this stepwise oceanic oxygenation process may have facilitated metazoan diversification and ecological expansion during Cambrian Age 2–Age 4. More broadly, despite a surge in redox work over the past decade, our study highlights the need to continue to develop sedimentary geochemistry databases.

ACKNOWLEDGMENTS

We thank Zihu Zhang and Wei Shi for laboratory assistance and Lidya G. Tarhan for helpful edits. This study was supported by the Chinese 973 Program (grant 2013CB955704), the National Key Research and Development Program of China (grant 2016YFA0601100), and the National Natural Science Foundation of China–Research Councils UK–Natural Environment Research Council Program (grant 41661134048).

REFERENCES CITED

Algeo, T.J., and Maynard, J.B., 2004, Trace-element behavior and redox facies in core shales of Upper Pennsylvanian Kansas-type cyclothems: Chemical Geology, v. 206, p. 289–318, doi:10.1016/j.chemgeo.2003.12.009.

Boyle, R.A., Dahl, T.W., Dale, A.W., Shields-Zhou, G.A., Zhu, M., Brasier, M.D., Canfield, D.E., and Lenton, T.M., 2014, Stabilization of the coupled oxygen and phosphorus cycles by the evolution of bioturbation: Nature Geoscience, v. 7, p. 671–676, doi:10.1038/ngeo2213.

Chen, D., Zhou, X., Fu, Y., Wang, J., and Yan, D., 2015a, New U-Pb zircon ages of the Ediacaran-Cambrian boundary strata in South China: Terra Nova, v. 27, p. 62–68, doi:10.1111/ter.12134.

Chen, X., Ling, H.-F., Vance, D., Shields-Zhou, G.A., Zhu, M., Poulton, S.W., Och, L.M., Jiang, S.-Y., Li, D., and Cremonese, L., 2015b, Rise to modern levels of ocean oxygenation coincided with the Cambrian radiation of animals: Nature Communications, v. 6, 7142, doi:10.1038/ncomms8142.

Erickson, B.E., and Helz, G.R., 2000, Molybdenum (VI) speciation in sulfidic waters: Stability and lability of thiomolybdates: Geochimica et Cosmochimica Acta, v. 64, p. 1149–1158, doi:10.1016/S0016-7037(99)00423-8.

Erwin, D.H., Laflamme, M., Tweedt, S.M., Sperling, E.A., Pisani, D., and Peterson, K.J., 2011, The Cambrian conundrum: Early divergence and later ecological success in the early history of animals: Science, v. 334, p. 1091–1097, doi:10.1126/science.1206375.

Jin, C., Li, C., Algeo, T.J., Planavsky, N.J., Cui, H., Yang, X., Zhao, Y., Zhang, X., and Xie, S., 2016, A highly redox-heterogeneous ocean in South China during the early Cambrian (~529–514 Ma): Implications for biota-environment co-evolution: Earth and Planetary Science Letters, v. 441, p. 38–51, doi:10.1016/j.epsl.2016.02.019.

Knoll, A.H., and Carroll, S.B., 1999, Early animal evolution: Emerging views from comparative biology and geology: Science, v. 284, p. 2129–2137, doi:10.1126/science.284.5423.2129.

Na, L., and Kiessling, W., 2015, Diversity partitioning during the Cambrian radiation: Proceedings of the National Academy of Sciences of the United States of America, v. 112, p. 4702–4706, doi:10.1073/pnas.1424985112.

Och, L.M., et al., 2016, Palaeoceanographic controls on spatial redox distribution over the Yangtze Platform during the Ediacaran-Cambrian transition: Sedimentology, v. 63, p. 378–410, doi:10.1111/sed.12220.

Okada, Y., Sawaki, Y., Komiya, T., Hirata, T., Takahata, N., Sano, Y., Han, J., and Maruyama, S., 2014, New chronological constraints for Cryogenian to Cambrian rocks in the Three Gorges, Weng'an and Chengjiang areas, South China: Gondwana Research, v. 25, p. 1027–1044, doi:10.1016/j.gr.2013.05.001.

Peng, J., Zhao, Y., Wu, Y., Yuan, J., and Tai, T., 2005, The Balang Fauna—A new early Cambrian fauna from Kaili City, Guizhou Province: Chinese Science Bulletin, v. 50, p. 1159–1162, doi:10.1360/982005-183.

Poulton, S.W., and Canfield, D.E., 2011, Ferruginous conditions: A dominant feature of the ocean through Earth's history: Elements, v. 7, p. 107–112, doi:10.2113/gselements.7.2.107.

Scott, C., and Lyons, T.W., 2012, Contrasting molybdenum cycling and isotopic properties in euxinic versus non-euxinic sediments and sedimentary rocks: Refining the paleoproxies: Chemical Geology, v. 324–325, p. 19–27, doi:10.1016/j.chemgeo.2012.05.012.

Smith, A.B., Zamora, S., and Alvaro, J.J., 2013, The oldest echinoderm faunas from Gondwana show that echinoderm body plan diversification was rapid: Nature Communications, v. 4, 1385, doi:10.1038/ncomms2391.

Sperling, E.A., Frieder, C.A., Raman, A.V., Girguis, P.R., Levin, L.A., and Knoll, A.H., 2013, Oxygen, ecology, and the Cambrian radiation of animals: Proceedings of the National Academy of Sciences of the United States of America, v. 110, p. 13446–13451, doi:10.1073/pnas.1312778110.

Sperling, E.A., Wolock, C.J., Morgan, A.S., Gill, B.C., Kunzmann, M., Halverson, G.P., Macdonald, F.A., Knoll, A.H., and Johnston, D.T., 2015, Statistical analysis of iron geochemical data suggests limited late Proterozoic oxygenation: Nature, v. 523, p. 451–454, doi:10.1038/nature14589.

Sperling, E.A., Carbone, C., Strauss, J.V., Johnston, D.T., Narbonne, G.M., and Macdonald, F.A., 2016, Oxygen, facies, and secular controls on the appearance of Cryogenian and Ediacaran body and trace fossils in the Mackenzie Mountains of northwestern Canada: Geological Society of America Bulletin, v. 128, p. 558–575, doi:10.1130/B31329.1.

Tarhan, L.G., Droser, M.L., Planavsky, N.J., and Johnston, D.T., 2015, Protracted development of bioturbation through the early Palaeozoic Era: Nature Geoscience, v. 8, p. 865–869, doi:10.1038/ngeo2537.

Yang, A., Zhu, M., Zhuravlev, A.Y., Yuan, K., Zhang, J., and Chen, Y., 2016, Archaeocyathan zonation of the Yangtze Platform: Implications for regional and global correlation of lower Cambrian stages: Geological Magazine, v. 153, p. 388–409, doi:10.1017/S0016756815000333.

Yuan, J.L., and Zhao, Y.L., 1999, Subdivision and correlation of Lower Cambrian in southwest China, with a discussion of the age of Early Cambrian series biota: Acta Palaeontologica Sinica, v. 38, supplement, p. 116–131 (in Chinese with English abstract).

Zhu, M.Y., 2010, The origin and Cambrian explosion of animals: Fossil evidence from China: Acta Palaeontologica Sinica, v. 49, p. 269–287 (in Chinese with English abstract).

Zhu, M.Y., Babcock, L.E., and Peng, S.-C., 2006, Advances in Cambrian stratigraphy and paleontology: Integrating correlation techniques, paleobiology, taphonomy and paleoenvironmental reconstruction: Palaeoworld, v. 15, p. 217–222, doi:10.1016/j.palwor.2006.10.016.

Manuscript received 3 October 2016
Revised manuscript received 6 April 2017
Manuscript accepted 23 April 2017

Printed in USA